AD-A183 871 VISIBLE FREE ELECTRON LASER OSCILLATOR(U) STANFORD UNIV 1/1
CA HIGH ENERGY PHYSICS LAB J A EDIGHOFFER ET AL.
JUN 87 N00014-85-C-0443

UNCLASSIFIED F/G 9/3 NL

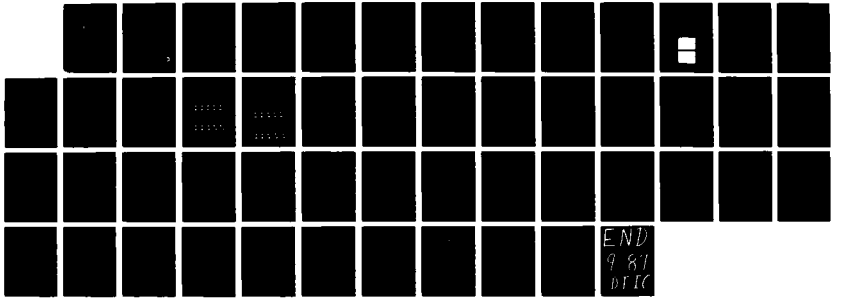

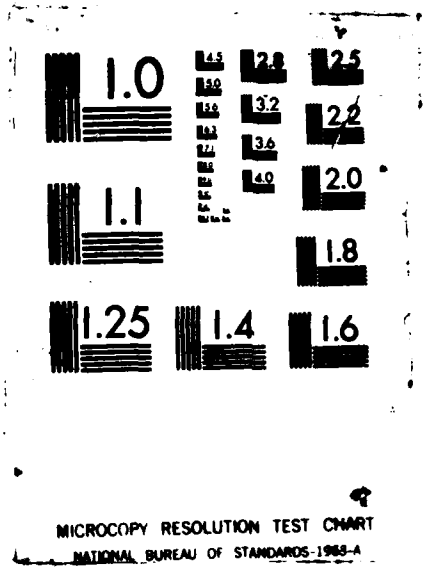

1112 13

Contract N00014-85-C-0443

TRW

VISIBLE FREE ELECTRON LASER OSCILLATOR

J.A. Edighoffer, G.R. Neil, S.W. Fornaca, H. Thompson

Applied Technology Division

TRW Space & Technology Group

One Space Park, Redondo Beach, Ca 90278

and

T.I. Smith, H.A. Schwettman, C.E. Hess, J. Frisch, V. Nguyen-Tuong, Y. LaPierre, R. Roghati

Stanford University

High Energy Physics Laboratory

June 1987

Final Report for Visible Free Electron Laser Program

Office of Naval Research

1030 East Green Street

Pasadena, Ca 91106

Table of Contents

Abstract 2

I. Experiment Purpose and Goals 2

A. Background 2

B. Visible FEL 4

II. Preparations for Lasing 4

A. Accelerator Modifications 5

1. Subharmonic buncher 5

2. Recirculation loop 6

3. High energy bunch diagnostics 10

B. Wiggler Modifications 10

1. Degraded performance.....11

2. Repair 11

3. Quadrupoles to erect beam 12

C. Resonator Modifications 12

1. High Q Optical Cavity 12

2. Cavity Stabilization 13

a. Angular Stabilization b. Length Stabilization

D. Optical Diagnostics 23

1. Power and Time-Averaged Spectra 24

2. 3rd Harmonic Power 24

3. Single-Shot Spectrum 24

4. Optical Quality 24

5. Pulse Length (Auto-Correlation) 25

III. Experimental Results.....25

IV. Appendix A 41

- Final Report on the Stanford University Subcontract

ABSTRACT

The first visible linac free-electron-laser(FEL) oscillator has been operated above threshold at the wavelength of 526 nm with and without a taper. Peak output power of 170KW with a macropulse average power of 1.1 watts was observed. The cavity dielectric mirrors were damaged at approximately 140KW/cm^2 of average power in the presents of UV from the FEL harmonics. The gain and efficiency were much less than predicted due to developed wiggler field errors.

1. Experiment Purpose and Goals

A. Background

In 1981, TRW measured the first optical gain in a tapered wiggler at EG&G, using the FEL as an amplifier on a CO2 laser. In 1982, TRW did the first optical beam quality measurement of the FEL optical beam quality, proving the beam was near diffraction limited.

In 1983, TRW's Free Electron Laser (FEL) Program at Stanford University's High Energy Physics Laboratory was the first to demonstrate oscillation in a tapered wiggler FEL.

Among the several interesting physics results that came out of that program were the observation of simultaneous two-frequency lasing (fundamental and third harmonic). Until 1987, that program held the United States record for short wavelength output (1.6 microns) and the world record for average FEL output power (80 watts).

In 1984, work proceeded to carry the laser output into the visible range, using relatively few hardware modifications to the Superconducting Accelerator (SCA). By scaling the measurements from the 1.6 micron experiment to predicted performance at 0.5 microns, it was determined that FEL would require one ampere of peak current in the wiggler to have sufficient gain to oscillate at 0.5 microns. Since the SCA had produced that peak current earlier, albeit at lower energy, it was concluded that by using the existing Recyclotron to raise the beam energy visible lasing could be achieved.

The tests carried out in late 1984 and early 1985 were unsuccessful in raising the gain of the FEL above the resonator losses. Analysis revealed that the magnetic optics in the Recyclotron were almost certainly responsible for reducing the peak accelerator current below the lasing threshold by stretching the electron bunch. (This was only a supposition since diagnostics that could provide verification were not in place at that time).

B. Visible FEL

In February, 1987, the Visible FEL Program achieved lasing in the green (0.525 microns) through combined modifications to the optical resonator (decreasing the cavity losses a factor of six) and to the accelerator injector, beamline and diagnostics (resulting in a peak current of three amperes). This report summarizes in Section II the modifications made to the accelerator, wiggler, optical resonator and diagnostics subsystems that were required for visible lasing. The FEL physics results are presented and discussed in Section III.

In addition to the visible lasing effort, the contract included measurements to determine the stability properties of an electron beam in single-cell cavities of the new rounded large-aperture geometry. A description of this experiment and the results are included in Section IV.

II. Preparations for Lasing

This section documents the modifications made to the FEL subsystems that were required for lasing in the visible region of the spectrum. Included are the changes made to the SCA and the optical resonator to ensure crossing the lasing threshold, a discussion of the wiggler as it now exists and a description of the optical diagnostics in place at the time of the final accelerator run.

A. Accelerator Modifications

The modifications that were made to the accelerator include the addition of a subharmonic buncher to the existing injector, a complete replacement of the recirculation system and the addition of a diagnostics system to determine electron beam bunch length at high energy. These changes permitted the production, maintenance and verification of high peak current bunches at the FEL.

1. Subharmonic buncher

To increase the amount of charge in a single RF bucket, a subharmonic buncher (SHB) was added to the injector of the SCA. The buncher operates at 236 MHz, the 11/2th subharmonic of the 1300 MHz fundamental frequency of the accelerator.

The SHB takes the long pulses originating from the fast gun pulse and coalesces them into a single fundamental RF bucket instead of throwing the ends away on the chopper. This causes the net (usable) charge per pulse from the injector to increase by about 100%.

2. Recirculation loop

The original four-pass recirculation loop for the SCA was designed with nuclear physics measurements in mind. In such experiments, the charge on target is the important parameter and no particular effort was expended in minimizing the bunch spreading. The original magnetic optics had a large T655 term (TRANSPORT notation for final energy as a function of the square of the initial length), which interacted with the large R56 term (final length as function of initial energy) to cause an increased bunch length. The facts that the initial bunch is of finite length and that a single-frequency accelerator imparts a cosine energy dependence on the beam meant that the optics would always cause bunch lengthening in that recirculation loop and the peak current would always drop when the recirculation loop was used.

For the free electron laser, the peak current is the quantity of prime interest. In the proposal, two methods were presented for dealing with the lengthening problem. The initially preferred method was to take the beam from the accelerator as it then existed, add a position-correlated energy spread to the bunch and run it through a magnetic dispersion module to erect the energy/phase ellipse. This method would attain the necessary peak current at the expense of the beam energy spread, but the SCA has a large margin in this regard.

The second approach, elimination of the problem at its source, was the one eventually chosen. The recirculation loop was completely replaced. The magnetic optics were redesigned from scratch, and optimized for the FEL application. The new optical system is shown in Figure A. It was installed and tested in the July, 1986, accelerator run; final adjustment to the magnet alignment was completed in the February, 1987, visible FEL run.

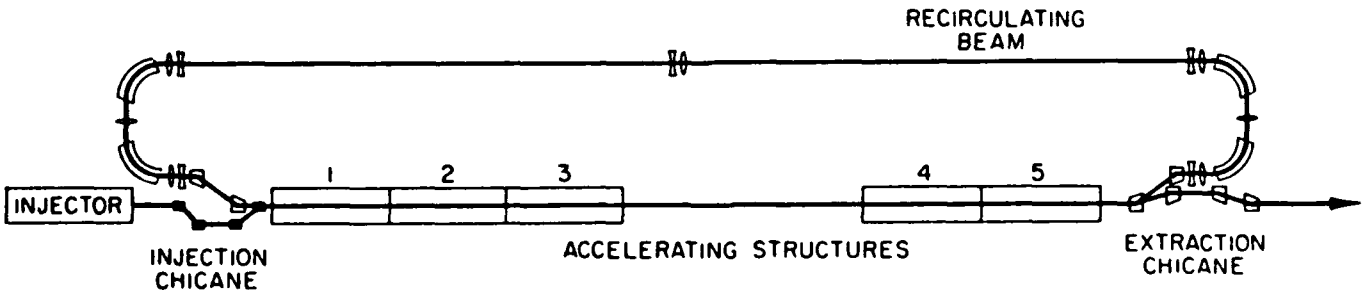

Figure A: BEAM RECIRCULATION SYSTEM

Energy recovery, an important (for FELs) off-shoot of the recirculation scheme, was documented during the July, 1987, checkout of the new recirculation loop. When the accelerator is operated in its normal mode (as a recyclotron), the recycled beam travels an integral number of RF wavelengths when returning to the front of the accelerator; the beam enters the structures at the same phase as it did on the first pass and the same increment of energy is added on the second pass through the structures.

If the path length is changed by an odd multiple of half wavelengths, then the recycled beam arrives 180o out of phase with the first beam. In this case the energy extracted from the RF field by the beam on its first pass is returned to the RF field by the beam on its second pass. There is no net flow of power since the electrons only "borrow" the energy for a while; the accelerator acts as a flywheel in this energy recovery mode.

The data for the energy recovery demonstration is shown in Figure 8. The traces are the difference of the power incident on and reflected from the cavity, i.e. the net klystron power used by the cavity in maintaining the acceleration field and powering the beam.

In the top figure, the accelerator is operated in the recyclotron mode. The beam absorbs power as it is accelerated on the first pass. In this experiment, some of the current (about 5%) was lost in the return loop, so the second pass absorbs only 95% as much power as the first

pass. The net two-pass power is 1 + 0.95 = 1.95 times the single pass power.

In the bottom figure, the accelerator is operated in the energy recovery mode by extending the path length of the return loop one half wavelength. Again, 5% of the current was lost in the return loop, so the remaining beam returned only 95% of the RF energy that it removed from the structures. The net two-pass power is 1 0.95 = 0.05 times the single pass power. Evidence of regenerative beam breakup was seen under certain conditions during this set of experiments.

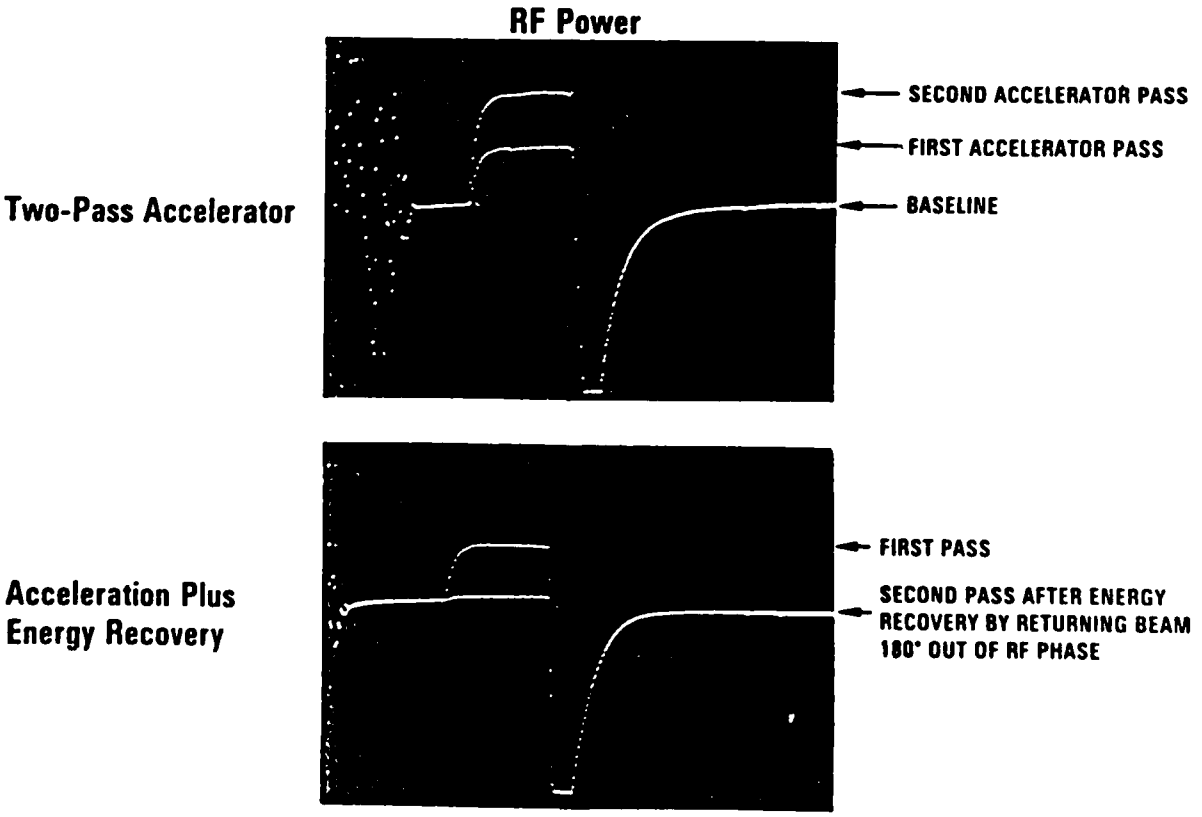

Figure B

3. High energy bunch length diagnostic

The original bunch length measurement system was at the low energy end of the accelerator. To check the bunch length after the beam was recirculated, it was necessary to add a nine-cell deflection cavity before the wiggler. It is operated by placing the center of the pulse at the zero-crossing of a magnetic dipole mode. The ends of the pulse receive an impulse from the non-zero magnetic field of the mode. The effect is seen after a long drift to a viewing screen, where the difference in transverse momentum from the front to the back of the pulse is transformed to a spread in position. Because the beam energy is high (the beam is stiff) and the pulse is short, very high peak fields are required in the cavity to cause sufficient deflection.

B. Wiggler Modifications

No modifications to the wiggler were planned originally, since the performance observed in the 1.6 micron experiments was consistent with predictions. However, during the November, 1986, checkout run it was found that the FEL gain had dropped by a factor of eight from the 1983 run. This was subsequently found to be due to changes in the wiggler fields.

1. Degraded performance

When the wiggler was installed, the magnetic field was measured and trimmed. The net root-mean-square deviation from uniformity was less than 0.7 %. When the field was remeasured following the November run, 6 % errors in the field were found. Large areas of the wiggler had degraded field profiles. Although some individual permanent magnets had been replaced over the three-year period, there was no obvious correlation between these locations and the bad zones. The cause of the deterioration is unknown, but one hypothesis is that it is due to effects originating with the electron beam, i.e. either radiation damage or heating the magnets beyond their reversible range.

2. Repair

To effect a quick fix, 15 wavelength sections were shimmed to bring the wiggler back to a more uniform field. This brought the RMS error to about 2.5 % (see Figure 8c). This level of error, while still a factor of 4 to 5 higher than the FEL energy acceptance of $1/2N = .5\%$, was sufficient to allow lasing in the green.

In the long term, any follow-on experiments will require the wiggler to be rebuilt in order to meet the 0.7 % error specification. An analysis of the individual magnets might reveal the cause of the wiggler field deterioration.

3. Quadrupoles to erect beam

One final minor modification was made to improve beam overlap in the wiggler. The original transport system caused the beam ellipse to be delivered to the wiggler entrance with its axis rotated with respect to the wiggler axis. This problem was alleviated by adding two quadrupoles upstream with their axes also rotated. When these quadrupoles were energized, the ellipse at the wiggler entrance was erected.

C. Resonator Modifications

Two major modifications were made to the optical resonator subsystem. First, the resonator mirrors were replaced with mirrors of higher reflectivity. Second, the stability of the resonator was improved.

1. High Q Optical Cavity

New mirrors were ordered for the resonator. These mirrors had a higher reflectance (0.9997 versus 0.996 for the old mirrors) and a slightly smaller radius of curvature (6.3 m versus 7.5 m for the old mirrors). The mirrors were measured both with a spectrophotometer and with the Deacon Research Q-measuring system. The latter yielded a

reflectivity Q in excess of 900. When the mirrors were installed in the experiment, an argon ion laser was used to make a cavity ring-down measurement of the Q. The result was a Q in excess of 600 at the argon wavelength of 0.5145 microns; when account was taken of the difference in mirror reflectivity between 0.51 and 0.53 microns, this value scaled to a sufficiently low loss resonator to attempt visible lasing. Ring-down measurements made during the visible lasing run showed the Q was actually 750.

2. Cavity Stabilization

a. Angular Stabilization

It was found during the 1.6 micron experiments that angular motion of the resonator mirrors was not a problem. Nonetheless, the resonator mirrors were repositioned on the optical tables to lie directly over the "point support" location, thereby minimizing the possibility of transverse movement. The high-gain angular feedback system installed for the long-wavelength experiments had little effect, and so was not used for the visible experiment.

b. Length Stabilization

From the initial attempts at visible lasing in 1984, it was clear that longitudinal motion of the mirrors would be

an issue. The high Q of the resonator (of order 1000) plus the short electron bunch L (about 1 mm) meant that the length of the resonator had to be held to L/Q of about 1 micron. The two resonator mirrors were located on separate optical tables, and the helium refrigerator directly over the experimental area generates ground motion that couples to the tables, causing them to move relative to each other.

One solution to this problem, and the one usually taken, is to sense the mirror motion and to feed an error signal back to move the mirror to compensate. As the mirrors become more massive and the mounts stiffer, the frequency response of this scheme deteriorates. We adopted a different approach, which involved changing the accelerator master frequency to track the changes in the optical cavity. That is, in effect, the optical cavity becomes the Master oscillator. A description of both of these approaches follows:

In normal operation the cavity length is adjusted until the round-trip time of the optical pulses in the optical cavity is equal to the time between the filled buckets in the electron beam, minus the small amount needed to correct for lethargy effects. The round trip time of the optical pulses in the cavity, Top, is given by Top=2Lc/c, where Lc is the cavity length, and c is the speed of light. The time between electron micropulses, TB, is given by TB=1/fB=nB/f0, where fB is the injector repetition frequency, f0 is the

linac fundamental frequency, and nB is the number of accelerator buckets between the electron micropulses. Overlap occurs when Top=TB (see Figure C).

Stable Oscillator has Overlapping Pulses

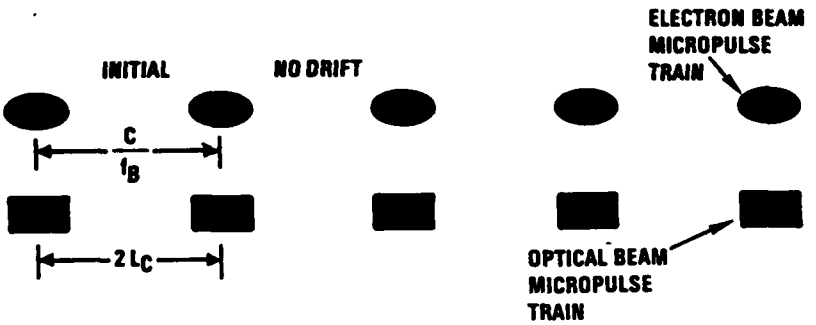

Mirror Drift ΔL Causes Loss of Overlap

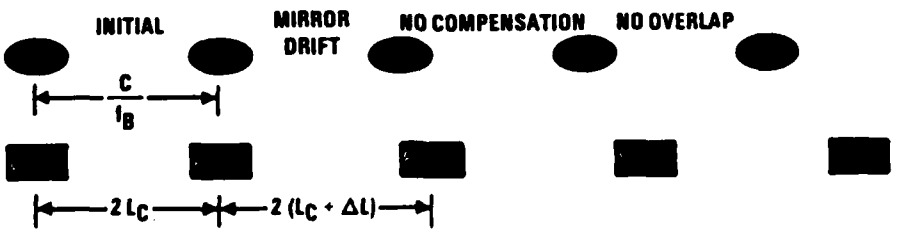

Figure C

In order to increase the operational stability of the FEL the length of the optical cavity may be stabilized against motions of the cavity end mirrors. These motions occur due to vibrations in the optical benches on which the mirrors are mounted, and due temperature variations. The cavity length may be adjusted by either of two methods: The cavity mirrors may be moved to return the cavity to its original length, or the accelerator fundamental frequency may be varied to maintain overlap based on the new cavity length (see Figure D).

Mirror Feedback δL Maintains Fixed Cavity Length ($\delta L = -\Delta L$)

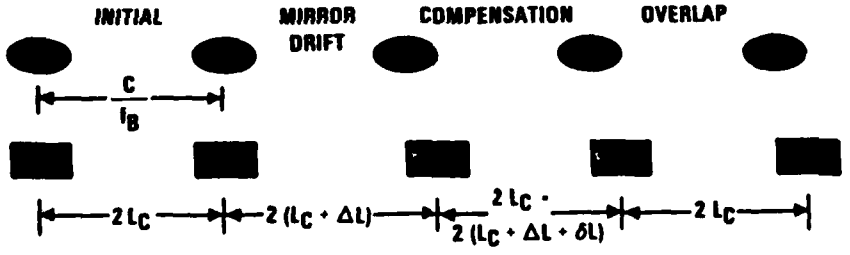

Frequency Feedback δf Maintains Fixed Overlap ($\delta f / f_B = -\Delta L / L_C$)

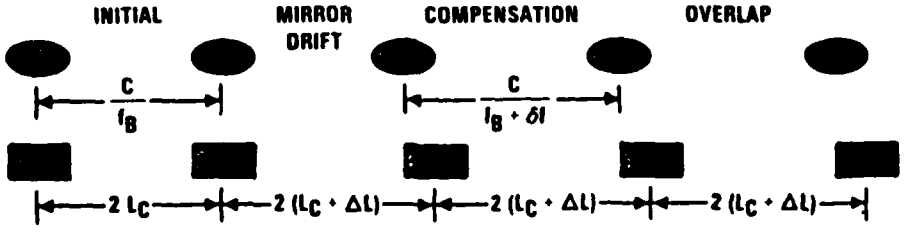

Figure D

The optical cavity length may be stabilized by mounting one of the cavity mirrors on a rapidly movable mount, such as a piezo-electric driven translation stage. The cavity length is then monitored with a interferometer, and when one of the mirrors drifts, changing the cavity length, the mirror position is changed to return the cavity length to its original value. The two disadvantages of this method is the difficulty or achieving the required range of motion and the appropriate frequency response.

Another approach to stabilizing the cavity length is to adjust the timing between the micropulses to adjust for the new optical cavity length after the end mirrors have drifted. The cavity length is again measured by using an interferometer, and when a change in the length is detected the inter-pulse timing is changed. One method of changing the timing would be to adjust the electron gun firing time of the injector. This is not a suitable method because it would change the relative phase between the acceleration field and the micropulse resulting in an energy variation. Another method of varying the inter-pulse timing is to change the frequency of the acceleration field in the linac. Varying the accelerator frequency has the advantage of maintaining the phase of the acceleration fields, and thus the electron energy, constant. This approach to length stabilization maintains the overlap between the electron and optical micropulses by adjusting the electron inter-pulse

time to be the same as the round trip time of the optical pulse with the new resonator length.

The amount of frequency adjustment, df, needed for a drift in the cavity length of dL is given by df/fB=-dL/Lc. The major advantage of this method of stabilization is that the frequency slew rate of the system is limited only by the settling time of the oscillator whose frequency is being varied, and therefore the feedback loop is faster than if the mirror was being moved. The disadvantage of this method is that the frequency slew is limited by the tuning width of the accelerator structures. The Q of the structures gives the tuning width since Q=f/df. The length error which can be corrected using frequency feedback is given by dl=Lc/Q.

The two methods of cavity length stabilization yield equivalent results. When the cavity mirrors are moved, the overlap between the electron and optical micropulses is maintained by keeping the cavity length fixed, and thus the time between the optical pulses fixed. Since the time between the electron micropulses is locked in this method, a fixed amount of overlap is maintained, with the only slippage due to the response time of the feedback loop. When the accelerator frequency is varied, the overlap between the electron and optical micropulses is maintained by varying the arrival time of the electron micropulses to coincide with the varying arrival time of the optical micropulses as the cavity length changes. The arrival time of the micropulses is directly changed by varying the

accelerator frequency, and a fixed amount of overlap may be maintained, with the only slippage due to the response time of the feedback loop.

The length stabilization system consists of four major subsystems: an interferometer for measuring the optical cavity length variations, a data link for transmitting the interferometer output to the computer, a computer for calculating the required frequency shift, and the master oscillator (see Figure E).

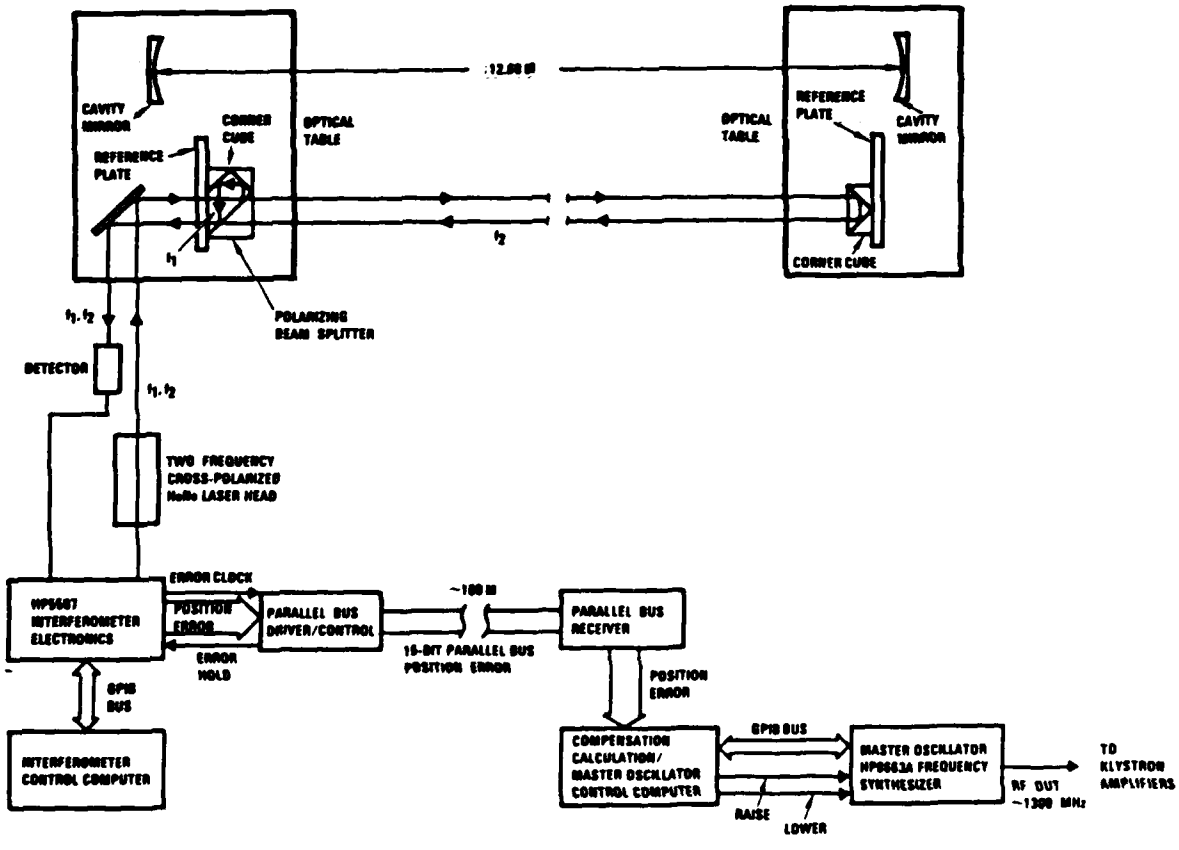

Figure E

The optical cavity length is measured using a Hewlett-Packard 5507 Interferometer. The optical cavity mirrors are mounted on separate optical tables. The distance between reference plates mounted on these tables is measured using the interferometer. Variations in this length are identical to variations in the optical cavity length under the assumption that there is no relative motion between the mirrors and the table. The interferometer uses a HeNe laser head which produces linearly cross polarized light at two frequencies f1 and f2. The beams are split using a polarizing beam splitter located at one reference plate. The beam of frequency f1 is directed into a corner cube mounted on the beam splitter and acts as the reference leg of the interferometer. The beam of frequency f2 is directed to a corner cube mounted on the other optical table. The two beams are then recombined on at the beam splitter and go to a detector which is sensitive to beating between the two frequencies. The interferometer is sensitive to length changes of 1/64 the wavelength of red HeNe laser light. The interferometer is initialized and controlled using a computer which communicates with the interferometer electronics via a GPIB bus. This computer is used to zero the interferometer, set the output data format, and reset the interferometer if the beam is broken.

There is a separation of about 160 m between the interferometer and the master oscillator, since the interferometer is located in the SCA tunnel at the FEL and

the master oscillator is located in the SCA control room. The link is provided by a 15 bit parallel data bus which transmits the position error signal from the interferometer to the computer which calculates the position error correction factors. The parallel bus is synchronous with the error clock of the interferometer electronics. The error clock is divide by 100, producing a position error update rate of 20 kHz on the data bus. While the data is being transmitted on the bus, the bus driver produces a signal which prevents the interferometer position error outputs from being updated. The position error is in twos complement format and has an accuracy of 1/64 the wavelength of HeNe light. The bus is differentially driven twisted pair to increase the noise immunity of the bus, and is terminated using differential line receivers. The position error data is stored in the parallel bus receiver so that it may be read asynchronously by the computer which calculates the error correction. The Error Hold bit also is transmitted by the bus to the receiver and is made available to the compensation correction computer. When this signal is true the position error is being updated, therefore the computer should not accept the data on the bus. The bus update rate is much faster than the rate at which the computer can read the data therefore conflicts are rare. The error position data is presented to the computer at the bus receiver as two bytes. The least significant bit of the low order byte is

the error hold signal and is not stored in the bus receiver, while the remaining 15 bits are the position error signal.

The position error signal is read into a computer which calculates the length variation and determines the required frequency shift. If the Error Hold bit of the input data is true the input data is ignored. The position error signal is converted into microns, and then the required frequency variation is calculated using the formula given previously, df=-dLf0/(Lc). For this case Lc is 12.68 m, and f0 is 1300 MHz, therefore a cavity length variation of 1 micron requires a frequency variation of 103 Hz. The frequency is compared to the previous value and if they are different the master oscillator is adjusted to the new value.

The master oscillator for the accelerator is a HP8663A Frequency Synthesizer. The center frequency and output power level of the master oscillator is set from the control computer via a GPIB bus and the control is passes to the auxiliary digital input connector. Before control is passed to the auxiliary input, the master oscillator is programmed to recognize raise and lower commands on the auxiliary input line to refer to frequency, and the frequency step size is programmed. The master oscillator frequency is then updated using the raise and lower lines of the auxiliary input. This is done because these lines have a faster response time then the GPIB bus, with the update time being limited only by the settling time of the synthesizer. In operation, the response time is limited by the speed at which the

compensation calculation loop is performed by the computer. The master oscillator frequency is adjusted in discrete steps, which can be varied. A nominal value used in the experiments was .2 Hz.

The Q of the SCA accelerator structures is such that the tuning range is 50 Hz. Therefore, the maximum length error which can be corrected is 46.6 microns. The error signal is averaged over one second and the long time variations are ignored, in order to keep the master oscillator frequency inside of the accelerator tuning range. Long term drifts in the cavity length are corrected by moving the cavity mirrors with motor driven micrometers

D. Optical Diagnostics

A number of optical diagnostics were prepared in anticipation of visible lasing. These included the "usual" diagnostics as developed in the long-wavelength experiments, such as total power and time-averaged spectra, plus various specialized set-ups to measure third-harmonic power in the ultraviolet region, single-shot spectra, time-averaged beam quality, and optical pulse length (using an autocorrelation measurement system in conjunction with Princeton University).

1. Power and Time-Averaged Spectra

A calibrated silicon diode was using to measure the average power, along with a phototube for comparison. The time-averaged spectra will be taken by scanning the grading of the spectrometer and average over many macropulses through a box car integrator.

2. 3rd Harmonic Power

The third harmonic of .5 microns is .133 microns, well in to the UV where it would not propagate through the atmosphere to the diagnostic area. A UV photodiode is therefore installed which can be inserted within the vacuum system though after the cavity mirror.

3. Single-Shot Spectrum

The single-shot spectra is to be taken by opening the exit slit on the spectrometer and focusing the output on to a silicon diode array. The array consists of 32 elements and focused so that each element spans .1% of the spectra.

4. Optical Quality

The optical quality setup was modified for visible operation. The involves viewing the FEL output spot size as

a function of the distance from a focus. By plotting the spot size verse distance from the focus, the beam quality can be determined independent of any optics errors.

5. Pulse Length (Auto-Correlation)

The autocorrelation experiment involves splitting and recombining the FEL beam and passing the resultant beam through a doubling crystal. By varying the path length of one of the split beams, the temporal overlap can be varied. Since by conversion efficiency is a function of peak power, the optical bunch length can be measure by measuring the converse efficiency as a function of this path length difference.

III. Experimental Results

Introduction

The free-electron-laser(FEL) has been demonstrated to be a versatile source of radiation in the infrared and visible region of the spectrum. Since the first FEL operation[1,2], it has been shown that the efficiency of energy conversion from the electrons to the optical field can be improved by tapering the wiggler field[3]. Three years

ago, we reported the first tapered wiggler oscillator results at 1.5 microns[4]. In this paper, we will present the initial results of extending operation of RF linac FELs to the visible.

An FEL generates stimulated radiation by the interaction of the relativistic electron beam with a transverse periodic magnetic field(wiggler). There is a resonance condition defined by the condition that an electron slips one optical period as it travels one period of the wiggler. This condition results in the electron transverse velocity always being in constant phase with the transverse optical electric field, so that as the electron's transverse motion reverses sign, so does the optical electric field seen by the electron. This gives the maximum integrated velocity dotted into the optical electric field(work done by or on), so that energy can be transferred from the electrons to the optical field.

The need for tapering arises because the resonance condition is energy dependent and therefore this resonance condition becomes a function of the position down the wiggler as the electrons lose energy to the optical beam. Tapering is done by changing the wiggler magnet field to maintain the resonance as the electron lose energy.

The well known resonant relationship is

$$\lambda_s = \frac{\lambda_w}{2\gamma^2}\left(1 + \frac{a_w^2}{2}\right), \quad a_w = \frac{qB_w}{mc^2}\frac{\lambda_w}{2\pi}$$

where λ_s is the optical wavelength, λ_w is the wiggler period, the electron energy is given by($E=\gamma mc^2$), q is charge of the electron bunch and Bw is the magnet field.

There is a range of initial electron phases which follow the tapered resonance condition; these electrons are said to be trapped in a potential well. The rest of the electrons are not trapped and do not remain resonant. The total efficiency of a tapered wiggler oscillator depends on the fraction of the electrons trapped and the average energy conversion of the resonant electrons[3].

Energy extraction measurements from electron beams in tapered wigglers using an external laser were demonstrated by several groups[5,6,7,8]. Tapered wiggler oscillators in the infrared have been demonstrated[4,9]. Orsay has generated visible lasing with an untapered klystron[10].

A 115 Mev electron beam is provided by the Stanford Superconducting Accelerator(SCA). The electron beam characteristics are shown in Table I.

ACCELERATOR PARAMETERS

Energy	**114.8 MeV**
Energy Spread	**.15%**
Emittance	**<15 mm mrad**
Average current (Macro)	**90μA**
Peak current (Micro)	**3 A**
Macropulse length	**1-5 ms**
Micropulse length	**3 ps**
Repetition Rate	**5 Hz**

Table I

1. Electron Beam

The electron beam used in the .5μ FEL experiment was provided by the Stanford Superconducting Linear Accelerator (SCA) and its beam recirculation system (Fig.X) which allows the electrons to be accelerated twice by the linac in order to achieve the necessary 115 MeV.

As details of the SCA have been provided elsewhere, the present discussions will be limited to descriptive material. The injector shown in Fig. X provides 5 MeV electrons to the rest of the system. It consists of a 100 keV gridded gun pulsed at an 11.8 MHz repetition rate. Electrons from the gun pass through an emittance filter and are bunched and chopped before injection into a pair of short superconducting structures. These structures further bunch the beam and increase its energy to 5 MeV. Current delivered by the injector consists of a train of pulses. Each pulse is typically 4° long (8 ps) and is separated by 84.6 ns (110 rf cycles) from the next pulse. The pulse train itself continues for milliseconds to 100's of milliseconds. The 4° pulse width can be adjusted by roughly a factor of two, while the longitudinal phase space required by the beam remains constant at about 40 keV-deg.

The main part of the accelerator consists of five identical superconducting structures, each powered by a separate 10 kw klystron. This set of structures is capable of adding 70 MeV to the beam, but for the purposes of the .5 μ experiment, the energy gain was set to 55 MeV. The quality of the beam from the injector is preserved in the linac, and feedback control of the fields assures an output beam of exceptional stability.

After exiting the linac, the 60 MeV electrons are guided by the recirculating transport system shown in Fig. back to the beginning of the accelerator. They are

reinjected and gain an additional 55 MeV, leaving the linac with a total kinetic energy of 115 MeV. A system of magnets labeled as"extraction chicane" on the figures automatically sends the 60 MeV electrons on their way back towards the beginning of the linac, while directing the 115 MeV electrons out of the loop and towards the FEL wiggler.

In addition to transporting the 60 MeV electron beam back to the beginning of the linac, the recirculation system was designed to be used as part of a magnetic bunching system in order to compress the beam bunch into as short a time as reasonable. Since the bunch change is conserved, the peak current rises due to the bunching and the gain of the FEL is increased. The magnets in the recirculation system provide a net dispersion of about 23° per percent energy spread. With this dispersion if the electron beam is phased on its first pass through the linac so that there is an appropriate correlation between the energy gain of an electron and its position within the bunch, the bunch will be compressed by the transport system. Any remaining energy-position correlation can be removed during the final pass through the linac.

Figure Y shows the results of measurements taken to determine the electron beam pulse length. The traces in both halves of the figure represent secondary emission current measured in a curve as the electron beam is scanned across the wire. The trace is thus a measure of the width of the beam. Upstream of the wire the beam passes through a microwave cavity driven at the linac frequency, but in a deflecting mode. The phase of the drive is chosen so that electrons at the center of the bunch receive no deflection, while those ahead of, or behind, the center will be deflected proportionally to their distance away from the center. As a result, the size of the beam at the wire is a function of the beam length in

the cavity. The two traces int the lower picture of Figure Y show the beam at the wire with the cavity powered, but with a phase shift of the cavity fields by 2° between the traces. The trace in the upper part of the figure shows the beam width with no fields in the cavity, and is necessary to understand the resolution limit of the measurement. Clearly, if the undeflected beam is too large, the effect of the cavity fields will not significantly change the beam size, and very little information will be obtained. Assuming that the effects of the undeflected beam affects the resulting size of the deflected beam in quadrature with the beam length, the length of the beam pulse in Figure Y can be determined to be 1.5° (3.2 ps).

The time averaged beam current delivered to the FEL was typically 100 μA. As this current is delivered as a train of 3.2 ps pulses separated by 84.6 ns, the peak current is 2.6 A. The measured energy spread on the beam is less than 0.1%, while the normalized transverse emittance was less than 5π mm mr.

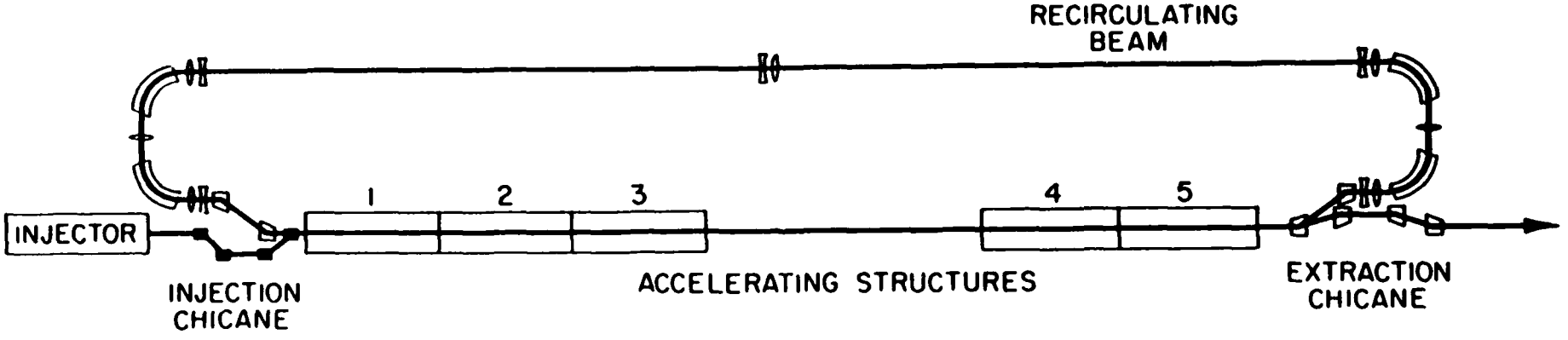

Figure 1: BEAM RECIRCULATION SYSTEM

Figure X

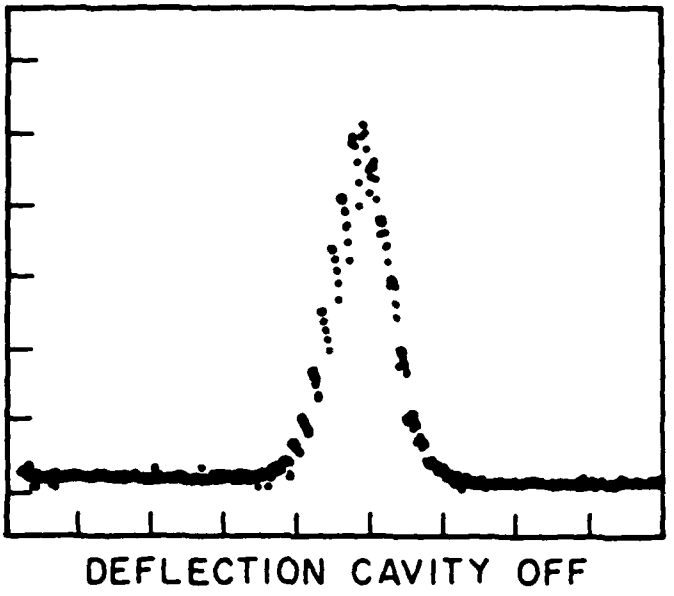

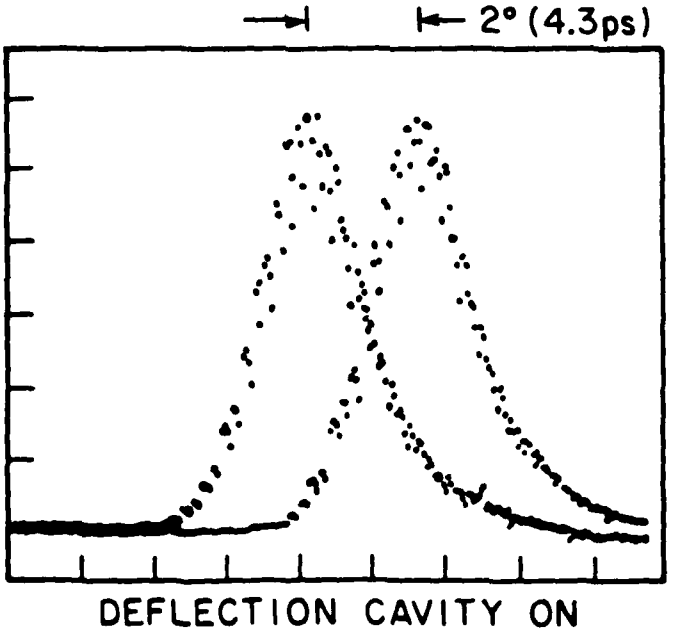

Figure Y

The experimental setup is shown in Fig. 1. The optical cavity consists of spherical dielectric mirrors 12.68 meters apart, centered on the wiggler; they are 8.0 meters radius of curvature and are 300 parts per million transmissive and 350 parts per million loss (scatter and absorption) at the wavelength of 525nm.

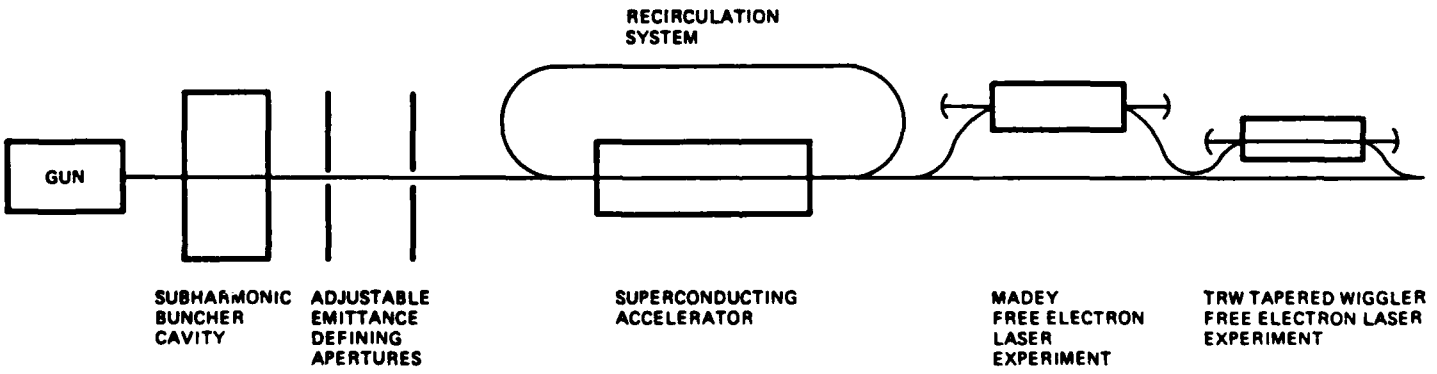

Figure 1

The wiggler is eight section of linear pure SmCo permanent magnet section plus a dispersion section, see Fig.2. Each section contains 15 3.6 cm periods with peak axis field of 2.9 kG. The taper is controlled by the gap spacing. The first and last section perform like an optical klystron at low optical powers, while at high powers, the first section becomes a prebuncher, enhancing the trapping fraction in the tapered section. The magnetic dispersion section has a controllable dispersion to optimize the trapping fraction.

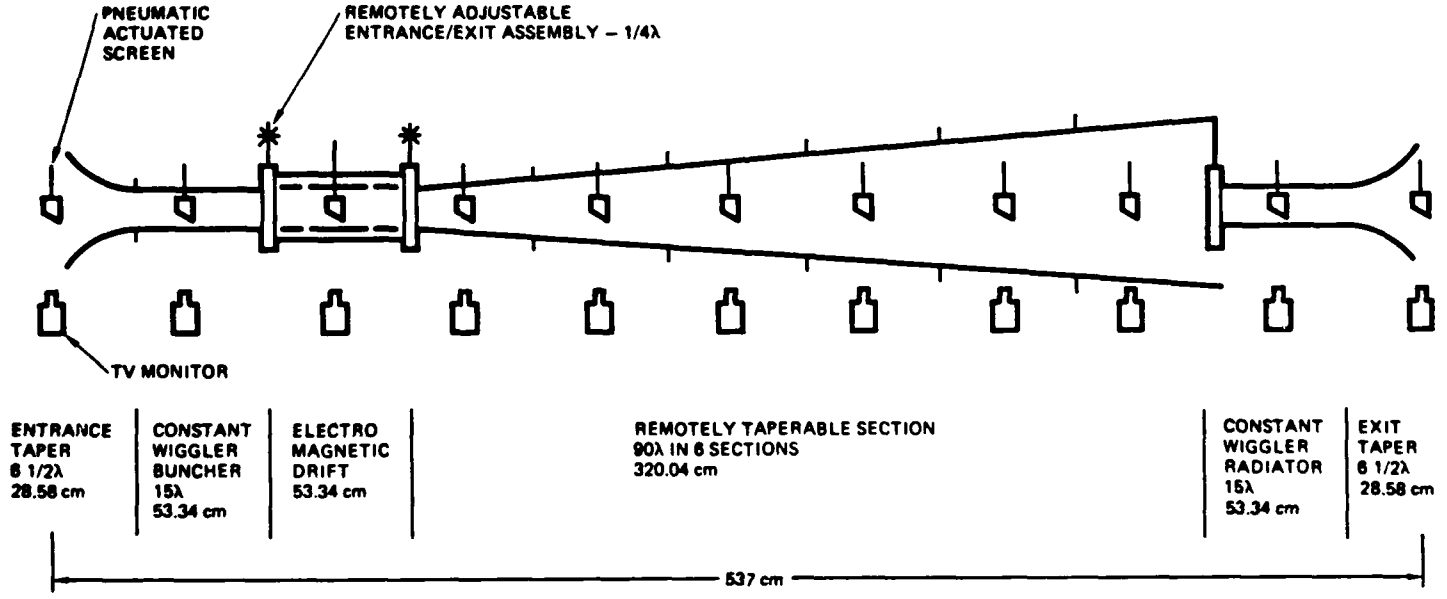

Figure 2.

The characteristics of the oscillator are listed in Table II. The wavelength was measured to be 525nm with a base to base width of 4 nm. The small signal gain for the constant wiggler was measured to be .5% which is factor 10 smaller than predicted. This is probably due to wiggler field errors which have increases from 1/2% RMS peak field errors to 4% for the current experiments. This is roughly the same as increasing the energy spread of the electron beam to 40% which is 8 times the energy acceptance of the FEL. This accounts very well for the lost gain and efficiency. The wiggler errors have increased due to thermal history effects, glue and reglueing history effects and radiation damage. The relative effects on the total error is being investigated.

The efficiency of the FEL was .03% for the constant and .05% for the 1% taper. These were again a factor of 10 to 20 below predicted values, which is again within range of the wiggler error effects.

The detuning curve was measured at 2 microns; that is the cavity length had to be exactly the right length within 2 microns. This leads to a stability problem as we observed a 5 micron motion at 16hz driven by the large mechanical pumps of the accelerator's helium refrigerator. The vibrations reduced lasing to every third or fourth accelerator macropulse.

LASER PARAMETERS

	Constant	Tapered (1%)
Wavelength	525 nm	525 nm
Spectral width	4 nm	
Gain	.5%	
Efficiency	.03%	.05%
Cavity Q	770 (round trips)	770 (round trips)
Output power (macro)	.8 W	1.1 W
Output power (micro)	120 Kw	170 Kw
Peak cavity power	190 Mw	260 Mw
Mirror Flux Density (macro)	100 Kw/cm^2	140 Kw/cm^2
Mirror Flux Density (micro)	2.2 GW/cm^2	3.0 GW/cm^2

Also observed was evidence of the "walking mode" first observed by Los Alamos[3]. This is observed, Fig. 3., in the ring down of the optical cavity after the accelerator pulse is finished. The ring down instead of being a simple exponential decay, has an oscillating structure superimposed on the decay. The explanation proposed by Los Alamos, in which we concur, is that there is a lensing effect from the FEL in the cavity only in the forward direction. If the lens is off center(electron beam misalignment) then this lens will also steer. There will be a distortion of the cavity mode while lasing that will "walk" back to the empty cavity mode after the electrons(lens) is removed. This causes the beam to walk back and forth across the aperture of the detector generation the ringing in the decay. This is indirect evidence for "optical guiding", in which the FEL interaction guides(focuses) the optical mode.

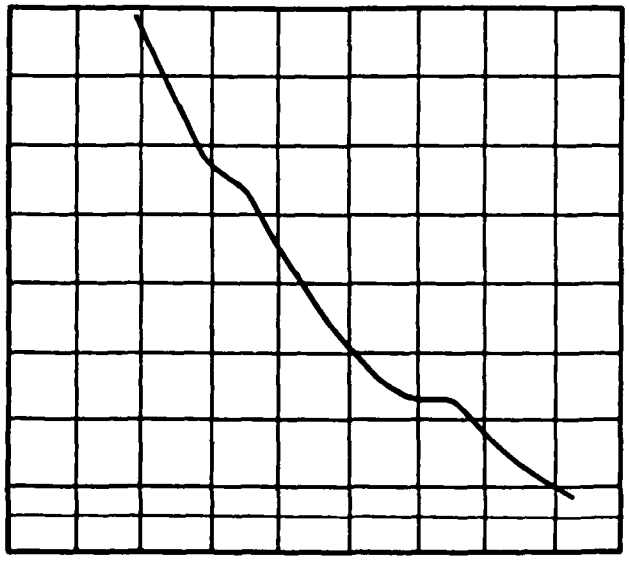

Figure 3

This was the first observation of electron linac FEL lasing in the visible with and without tapering. Accumulated wiggler errors since its original installation have cause severe performance degradation from the 1.6 micron experiment of 1983[4]. Also, some indirect evidence for optical guiding was observed.

1) J. M. J. Madey, H. A. Schwettman, and W. M. Fairbank, IEEE Trans. Nucl. Sci. 20, 980 (1973).

2) D. A. G. Deacon, L. R Elias, J. M. J. Madey, G. J. Ramian, H. A. Schwettman, and T. I. Smith, Phys. Rev. Lett. 38, 891 (1977).

3) N. Kroll, P. Morton, and M. Rosenbluth, IEEE J. Quantum Electron 7, 89 (1980).

4) J. A. Edighoffer, G. R. Neil, C. E. Hess. T. I. Smith, S. W. Fornaca, and H. A. Schwettman, Phys. Rev. Lett. 5, 344 (1984).

5) H. Boenmer, M. Z. Laboni, J. Edighoffer, S. Fornaca, J. Munch, G. R. Neil, B. Saur, and C. Shin, Phys. Rev. Lett. 48, 141 (1982).

6) J. Slater, J. Adamski, D. Quimby, T. Churchill, L. Nelson, and R. Center. IEEE J. Quantum Electron 19, 391 (1982).

7) R. Warren, B. Newnam, J. Winston, W. Stein, L. Young, and C. Brau, IEEE J. Quantum 19, 391 (1983).

8) T. J. Orzechowski, B. R. Anderson, J. C. Clark, W. M. Fawley, A. C. Paul, D. Prosnitz, E. T. Scharlemann, S. M. Yarema, D. B. Hopkins, A. M. Sessler, J. S. Wurtele, Phys. Rev. Lett. 57, 2172 (1986).

9) D. W. Feldman, et. al., submitted to IEEE J. Quantum Electron (1987).

10) J. Billardon, P. Elleaume, J. Ortega, C. Bazin, M. Velgne, Y. Petroff, D. Deacon, K. Robinson, and J. Madey, Phys. Rev. Lett. 51, 1652 (1983).

IV. Appendix H

- Final Report on the Stanford University Subcontract

Report on SCA Beam Recirculation

The beam recirculation system on the SuperConducting Accelerator has been rebuilt in order to satisfy the short pulse requirement of the 0.5 micron free electron laser experiment. The problem and its solution are both described below.

Beam recirculation is necessary to obtain the 115 MeV energy required for 0.5 micron FEL operation. Initial 0.5 micron experiments in 1984 failed because the length of the electron bunch increased while going through the recirculation system, causing the peak electron current to drop below the threshold for FEL oscillation. There is an unavoidable second order spread in beam energy caused by the time-varying fields in the accelerating cavities (T655 in TRANSPORT[1] notation). The non-isochronous recirculation system (R56 non-zero, in TRANSPORT notation) converts this energy spread into lengthening of the electron bunch. It is also possible to use the non-isochronous recirculation system to shorten an electron bunch, by introducing a head-to-tail energy variation along the electron bunch before it goes through the recirculation system. This energy variation can be produced by changing the phase of one or more of the accelerating structures. These two effects combine to permit a minimum bunch length, which was found both experimentally and by subsequent calculation to be about 8 picoseconds.

In order to solve this problem, a magnetic bunching system was initially proposed. This consisted of a four magnet chicane, each magnet being 40 cm long with a 5 kG field. The beam would be displaced by about a meter within the chicane. It was realized later that the bunch length problem could also be solved by rebuilding the beam recirculation system in such a way as to permit shortening the electron bunch length. This solution had a number of advantages over the magnetic buncher, including simpler magnet and beamline design, and wider apertures for the recirculating electron beam. Further the new recirculation system could be built to be translatable, permitting easy variation of the recirculation path length by 12 cm in order to do energy recovery experiments. For these reasons the magnetic bunching system was rejected in favor of a rebuilt recirculation system.

The new recirculation system is shown in Fig 1; each 180° bend consists of two 90° magnets with a central quadrupole. This configuration is doubly achromatic but not isochronous. The magnets have a bending radius of 60 cm and a field of 3 kG. The conversion factor from energy spread to bunch length (R56) for the new system is 1.5 cm per % energy change, which is a factor of 3 lower than for the old system. This system in fact permits the electron bunch to be compressed to a measured value of 3.1 ps, and was instrumental in the success of our recent 0.5 micron FEL experiment.

Report on the Beam Cavity Interaction Experiment

We report the first measurements of multibunch electron beam excitations on a single cavity made while tuning the cavity through resonance. Our aims were to learn how strong the multibunch excited fields are, what is necessary to control them, and how well experiment and theory agree.

Multibunch effects are important in FEL accelerators, storage rings and linear colliders, where the time interval between electron bunches is large compared to the RF period (so that higher order modes are likely to be nearly resonant with harmonics of the electron beam frequency) and short compared to the decay time of the beam induced fields. The beam induced fields may then resonantly build up to significant levels. The parameter that governs the resonant build-up is

$$\tau = \pi f T_b / Q$$

where f is the mode frequency, T_b is the electron beam period and Q is the quality factor of the mode. Multibunch effects are important if $\tau < 1$. The room temperature copper cavity used in our experiment has $\tau = 0.025$ for the TM011 mode. This shows that multibunch effects are important even for room temperature accelerators, and must be considered while designing the loading for the higher order modes.

The cavity used in this experiment was a room temperature 1.3 GHz copper CERN-type cavity shown in Fig 2. It is mounted in a fixture that permits axial elongation and compression for tuning purposes. The computer program URMEL[2] was used to calculate the cavity modes and their R/Q values. The cavity was set up on a bench and the mode frequencies and tuning rates (frequency change per unit increase in axial length) were measured. These data are shown in Table 1.

The cavity was installed on the beamline, with a probe to sample the fields. The sampling probe was connected to a spectrum analyzer. This measures the amplitude of the excited fields but not the phase. In general the excited normal modes of the cavity will not be exact harmonics of the electron beam frequency, and the steady state beam induced field will not be in phase with the electron bunches. Thus the beam induced voltage may be thought of as consisting of a real part (in phase with the electron bunches) and an imaginary part (90° out of phase). In general one is more concerned with the real part, because it causes the beam to lose energy to the cavity mode, but in fact the imaginary part can lead to beam focussing and can be important too.

The cavity was driven with an electron beam pulsing at 11.828 MHz (110th subharmonic) and several modes were identified and studied. The beam induced voltage was measured while compressing the cavity so as to vary the frequency of the mode under study. When the mode frequency is an exact harmonic of the electron beam frequency, the mode excitation is resonant and at its strongest. Figure 3 shows these excitation curves for two modes, one m=0 monopole mode and one m=1 dipole mode. Both measured power and calculated power are shown. The beam induced voltage is calculated in [3] and for a mode designated by subscript m is

$$\bar{V} = \frac{V_0}{2} \cdot \frac{1 + e^{-\tau_m + i\delta_m}}{1 - e^{-\tau_m + i\delta_m}}$$

where τ was defined above and δ is the phase shift of the excited normal mode between successive electron bunches (δ varies as the cavity is tuned). V_0 is the induced voltage due to a single short bunch of charge q,

$$V_0 = \pi f_m \left(\frac{R}{Q}\right)_m q$$

The outcoupled power is then

$$P = \beta I^2 \left(\frac{R}{Q}\right) Q \cdot \frac{\tau_m}{2} \cdot \frac{1 - e^{-2\tau_m}}{1 - 2e^{-\tau_m}\cos\delta_m + e^{-2\tau_m}}$$

where I is the average beam current and β is the coupling constant of the probe. The measured and calculated outcoupled powers at resonance are shown in Table 2; the agreement is quite good. The calculated curves in Figure 3 have been scaled to match the measured power at resonance, thus highlighting the agreement between the shapes of the measured and calculated curves. The excitation of the TM011 mode levels off away from resonance; this is thought to be the direct excitation of the probe by the electron bunches.

An attempt was made to search for high frequency trapped modes above the beampipe cutoff frequency. We did not find a resonant trapped mode with $(R/Q)Q > 1000$ up to 8 GHz.

In conclusion, we have measured multibunch effects while tuning the cavity through resonance and have demonstrated agreement between theory and experiment both for m=0 and m=1 modes. The prognosis for predicting multibunch beam excitation levels in future machines is therefore good. In our experiment no resonant and high-impedance trapped modes were found above the cut-off frequency.

References:

1. K L Brown et al, SLAC Report 91 (1974).

2. T Weiland and J Tueckmantel, DESY Report M82-07.

3. P B Wilson, SLAC Report 2884 (1982).

TABLE I. MEASURED AND CALCULATED PROPERTIES OF SEVERAL CAVITY MODES

Mode		URMEL				MEASURED		
		f[MHz]	Q	$\frac{R}{\theta}$ [Ω]	$(\frac{R}{\theta})' b^{2*}$ [Ω]	f[MHz]	Q	$\frac{\partial f}{\partial L}$ $[\frac{kHz}{mil}]^{\dagger}$
m=0	TM_{010}	1296.61	2.77×10^4	127		1296.60	2.88×10^4	+65
	TM_{011}	2346.14	2.80×10^4	44		2352.10		-19
	TM-0-EE-2	2751.88	4.02×10^4	0.46		2768.78	3.08×10^4	-64
	TM-0-ME-2	3482.14	3.42×10^4	9.0		3481.0		+20
m=1	TE_{111}	1743.24	3.45×10^4		10.4	1744.57	1.24×10^4	-175
	TM_{110}	1892.08	3.12×10^4		23.3	1888.98	1.34×10^4	+19
	1-ME-2	2644.29	2.57×10^4		16.4	2647.60	7.50×10^3	+45
	1-EE-2	2710.10	3.18×10^4		5.2	2707.00	8.63×10^3	-270

* This is R/θ for beam displacement equal to the beampipe radius

† L is the axial length of the cavity

TABLE 2: COMPARISON BETWEEN CALCULATED AND MEASURED OUTCOUPLED POWER AT RESONANCE

Mode	Outcoupled Power	
	Calculated	Measured
TM_{011}	-8.9 dBm	-10 dBm
TE_{111}	-23.3 dBm	-22 dBm

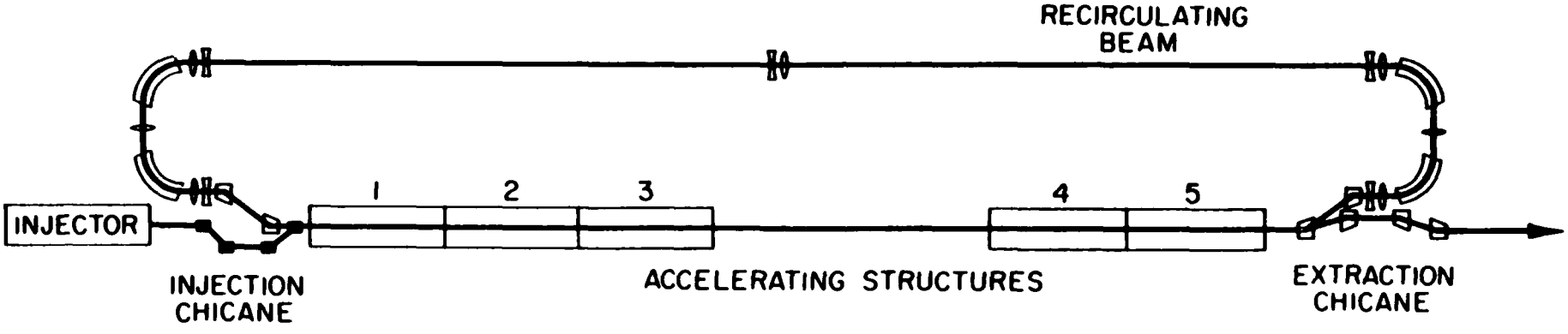

Figure 1: BEAM RECIRCULATION SYSTEM

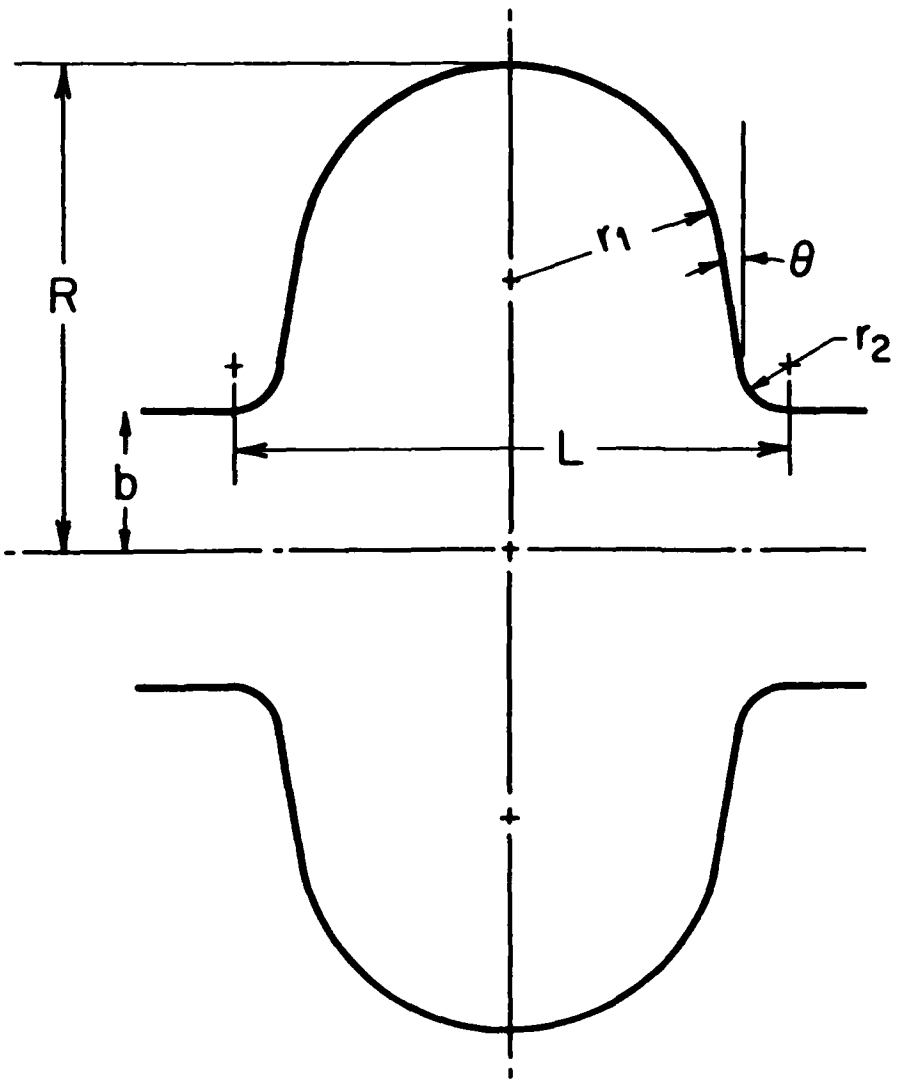

Cavity Dimensions	
R	10.14 cm
b	3.175 cm
θ	10.5°
r_1	4.557 cm
r_2	1.016 cm
L	11.852

Figure 2: CAVITY GEOMETRY

Figure 3: OUTCOUPLED POWER AS A FUNCTION OF MODE FREQUENCY

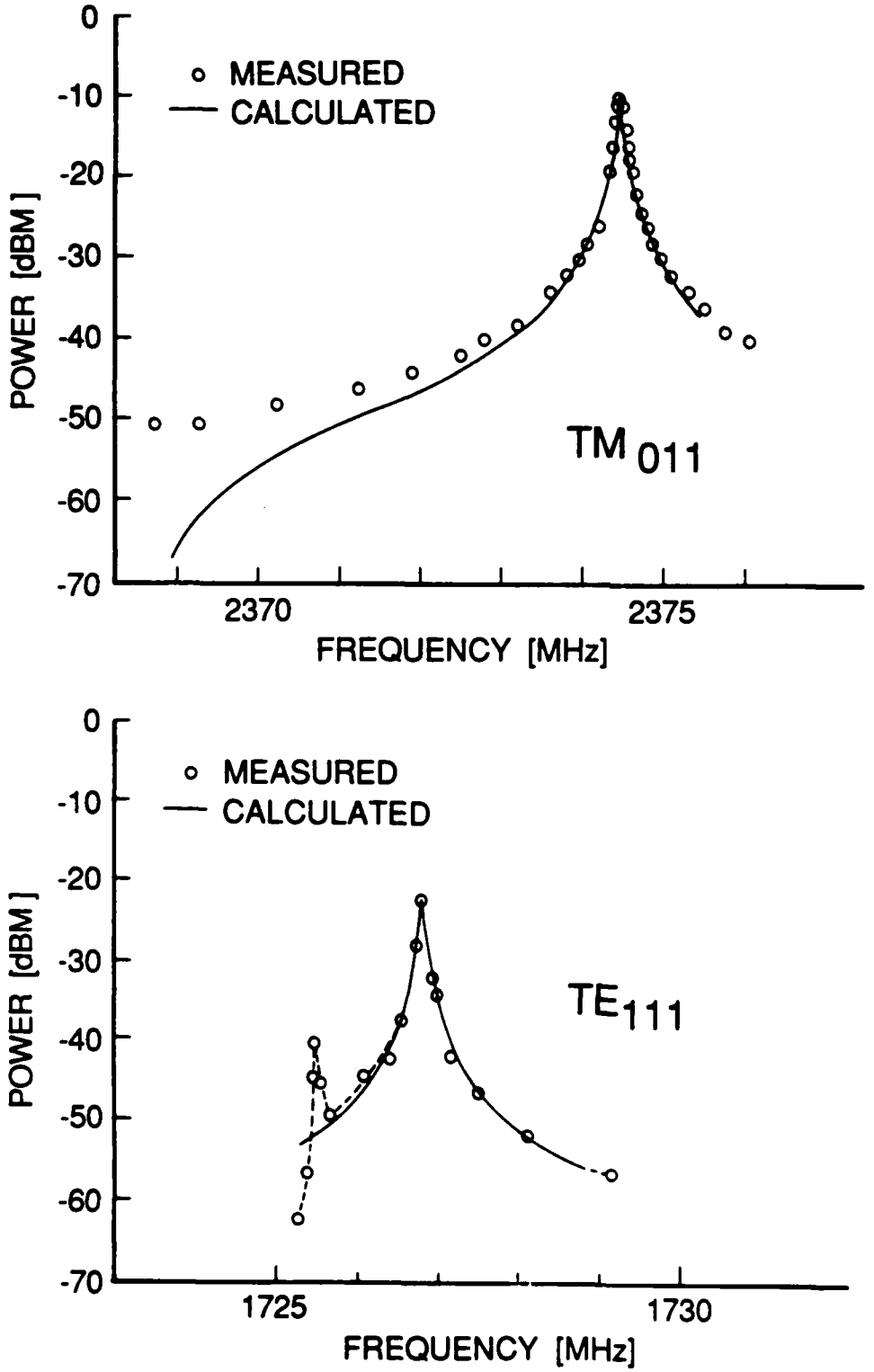

END

9-87

DTIC